Lawrence Berkeley National Laboratory
Recent Work

Title
SEMICONDUCTOR DETECTOR X-RAY FLUORESCENCE SPECTROMETRY APPLIED TO ENVIRONMENTAL AND BIOLOGICAL ANALYSIS

Permalink
https://escholarship.org/uc/item/2ch7h6d0

Author
Jaklevic, Joseph M.

Publication Date
1972-03-01

SEMICONDUCTOR DETECTOR X-RAY FLUORESCENCE SPECTROMETRY APPLIED TO ENVIRONMENTAL AND BIOLOGICAL ANALYSIS

Joseph M. Jaklevic and Fred S. Goulding

March 1972

DISCLAIMER

SEMICONDUCTOR DETECTOR X-RAY FLUORESCENCE SPECTROMETRY APPLIED TO ENVIRONMENTAL AND BIOLOGICAL ANALYSIS*

Joseph M. Jaklevic and Fred S. Goulding

Lawrence Berkeley Laboratory
University of California
Berkeley, California 94720

SUMMARY

The effective application of Si(Li) semiconductor X-ray detectors to the elemental analysis of trace impurities in environmental and biological specimens has required the improvement of existing systems. The use of low-background X-ray tubes for fluorescence excitation and the increased counting rate capability of the electronics have reduced counting times necessary for analysis. The presence of radiation-induced low-energy background in conventional detectors has been shown to be a major limiting factor in the detection sensitivity for trace element constituents in organic specimens. The use of guard-ring detector geometries has eliminated the cause of much of this background, and has reduced detection limits by approximately an order of magnitude. The practical detection of 0.1 ppm concentration achieved with these techniques has made energy-dispersive X-ray fluorescence a potent tool for the analysis of environmental and biological samples. A few examples have been chosen to emphasize particular advantages of the technique relative to alternative analytical methods. Examples include trace element determination in blood, air pollution particulate analysis, and studies of the influence of environment on the trace constituents of biological specimens.

INTRODUCTION

In this paper we discuss certain instrumental aspects of X-ray
fluorescence analysis with semiconductor detectors, and relate these
to some specific analytical applications. To facilitate the explana-
tion of these ideas, we will review some elementary concepts concern-
ing the X-ray fluorescence method and, in particular, our adaptation
of it to analysis of trace elements.

X-RAY FLUORESCENCE TECHNIQUE

The technique of X-ray fluorescence (shown schematically in Fig.
1) involves the excitation of the sample to be analyzed with particles
or X rays of sufficient energy to eject inner shell electrons from the
atoms in the sample. The atomic orbital vacancies produced are then
filled by the transition of electrons from higher energy orbits with
the accompaning emission of X rays. Each X-ray energy is equal to the
difference in binding energy between the two atomic orbits involved
in the process, and is therefore a characteristic of the atomic number.
These characteristic X rays are then detected by a system capable of
resolving the X rays from the different elements. Their intensities
are recorded in the form of a pulse-height spectrum and related to the
concentration of the various elements in the sample.

Although many processes can be used to produce the necessary
orbital vacancies, our work utilizes the photoelectric interaction of
incident monoenergetic X rays. X rays have the advantage that their
interaction mechanisms in matter are well understood and accurately
calculable--furthermore they can be easily produced either by radio-
isotopes or by electron beams in X-ray tubes. By comparison, direct
electron-beam excitation of the sample has the disadvantage that the

incident electrons also lose energy by emitting a continuous Bremsstrah-
lung spectrum of radiation which interferes with the characteristic
lines from the sample. This unwanted background decreases the detection
sensitivity for minor elemental constituents in the sample. Heavy
charged-particles (e.g. protons, alphas, etc.) have ionization cross
sections approaching those of X-ray excitation, and do not generate
appreciable Bremsstrahlung. However, arguments against their use
include the necessity for a particle accelerator, together with the
fact that in most practical applications monoenergetic X-ray tubes
achieve better detection sensitivities. Although charged particles
may possess advantages in certain applications, our experience is that
X-ray excitation constitutes the most sensitive and versatile means of
fluorescence analysis.

In addition to the photoelectric interactions which produce the
desired vacancies, incident X rays can also interact in the sample by
either coherent or incoherent scattering. In the coherent process,
the incident X ray is scattered without losing any energy. Incoherent
scattering refers to low-energy Compton collisions between the 'X rays
and free electrons. Only a small fraction of its initial energy is
lost by the X ray and no fluorescent X rays of any consequence result.
(This is in contrast with high-energy Compton processes where a size-
able fraction of the incident photon energy can be transferred to the
electron.)

Although these scattering processes do not contribute to the
fluorescence X-ray intensity, they play an important role in determin-
ing the sensitivity of the method particularly with respect to samples
consisting of light element matrices with trace concentrations of
heavier elements. Since this class of samples is particularly impor-
tant when considering trace-element contamination in environmental and
biological samples, it will be discussed in considerable detail. The
scattering is dominated by the light elements in the sample matrix,
whereas the fluorescence X rays of interest originate in photoelectric

interactions in the trace element atoms. Thus the final spectrum con-
sists of large backscatter peaks from the incident X rays, with the
characteristic fluorescent X-ray peaks superimposed on a background
distribution.

These features are illustrated in Fig. 2, which is a schematic
spectrum of the output from the X-ray spectrometer when such a sample
is irradiated by monoenergetic X rays. The prominent high-energy peaks
are due to coherent and incoherent scattering of the initial X rays in
the sample. By using monoenergetic X rays we confine the backscattered
radiation to the high-energy part of the spectrum. The presence of a
continuum of energies in the incident X-ray spectrum would result in a
continuum of scattered background which would obscure the fluorescence
peaks. The distribution of pulses at very low energies results from
Compton scattering of X rays in the detector itself. The X rays inci-
dent on the detector (mainly scattered from the sample) produce a con-
tinuum of electron energies in the detector up to a maximum determined
by the dynamics of the Compton process.

The interesting information is contained in the small peaks result-
ing from fluorescence of impurities in the sample. When the system is
properly calibrated the energy and intensity of these peaks can be
related to the concentrations of elements in the specimen. Since many
of the analytical problems of environmental interest concern the measure-
ment of minute quantities of impurity elements, it is important that
the system be able to measure these peaks in the presence of large-
amounts of scattering. The most recent improvements in semiconductor
X-ray spectrometry have been in the understanding and reduction of the
background induced in a spectrum by the scattered radiation.

Figure 3 shows some recent experimental results obtained in what
has now become a classic example of heavy-element environmental pollu-
tion--mercury in tuna fish. Comparison of these data with the schema-
tic spectrum of Fig. 2 serves to identify the various features of
interest in the spectrum. The slope in the background at higher ener-
gies results from sample scattering of the low-energy tail in the X-ray

tube output. Analysis of these data indicate a concentration of 2.0 ppm of Hg in the dried sample, which corresponds to a concentration of 0.4 ppm in the original tuna fish. The ability to simultaneously detect many elements present at such low levels in 10 min. counting times represents a new analytical capability, and one of great importance in environmental research and monitoring applications.

FACTORS AFFECTING SPECTROMETER PERFORMANCE

The ability to perform this type of measurement with semiconductor X-ray spectrometers is made possible by the many improvements in design which have occurred over the past few years. The ability to distinguish between X rays of similar energies is dependent upon the energy resolution of the Si(Li) spectrometers. The past three years have seen continuing improvements in this aspect of performance--energy resolutions have decreased from 300 eV at 5.9 KeV, to values of 145 eV currently reported. These improvements are of obvious importance, and are well known to anyone active in the semiconductor detector area over the past few years. Further reductions in electronic energy resolution will not significantly enhance performance since the region of most interest in analytical applications corresponds to X-ray energies greater than 4 keV. At these higher energies the total resolution becomes dominated by detector charge statistics.

The use of pulsed optical feedback systems has been instrumental in improving the rate performance while maintaining excellent energy resolution characteristics in spectrometers.[1] The related development of monochromatic, low-power X-ray tubes has made it possible to achieve counting rates with realistic sample geometries which are limited only by the spectrometer electronics.[2,3] These capabilities are required

to achieve the increased counting rates necessary to accumulate within a short period of time enough data to provide the necessary statistics to permit recognition of small fluorescence peaks.

The third area of importance which we discuss in detail in this paper concerns the background characteristics of the Si(Li) detector itself.[4] The limit in the analytical sensitivity of the system is determined by the low-energy background in the output spectrum. This can be related to degraded signals in the detector resulting from the detection of high-energy scattered X rays. Since most of the X rays observed by the detector fall in this class, only a small fraction of these events need be reduced in energy to produce a sizeable background.

THE GUARD-RING METHOD

Figure 4 is a fluorescence spectrum obtained from a blood serum sample using a conventional detector and excitation by monoenergetic characteristic Molybdenum X rays. The shape and height of the continuous background cannot be accounted for by simple physical mechanisms. Multiple scattering effects cannot be invoked to explain these partial energy losses since the energy transfer in scattering events at these energies is small; furthermore, the cross-section for photoelectric interactions in the detector is so much larger than the scattering cross-sections that the possibility of multiple scatterings is eliminated. Attention is therefore focused on mechanisms in the detector itself that cause the charge signal to be only partially collected for some fraction of the events.

In order to elucidate the mechanisms responsible for this background we have performed scanning measurements across the entrance window of a standard top-hat detector. The collimator aperture was

0.5 mm and could be positioned to within an accuracy of 0.1 mm. The
results are shown in Fig. 5. The top portion of the figure shows the
total efficiency (defined as the number of counts in the complete spec-
trum normalized to 1.0 at the center) for ^{55}Fe detection as a function
of position across the detector face, and serves to illustrate the
collimator resolution and to define the dimensions of the active volume.
A similar scan with a ^{109}Cd source gave virtually identical results for
the total detection efficiency. The half thickness in Si for absorption
of Mn Kα X rays produced by ^{55}Fe is only 0.02 mm whereas the half thick-
ness for the Ag X rays from ^{109}Cd is 0.7 mm. The Mn X rays sample only
the surface of the detector, whereas the Ag X rays interact over a
greater depth.

A very different result emerges when the efficiency for counts in
the photopeak only is measured. The lower curves show the ratio of the
K X-ray photopeak intensities to the total number of counts in the
spectrum. The scan with ^{55}Fe shows a reasonable uniform behavior over
the surface of the detector; however, with ^{109}Cd it is obvious that
there is a serious reduction in peak/total at the periphery of the
detector. Since the outer 1 mm of the detector diameter accounts for
1/3 of the active area of the device, a sizeable degradation in peak
to background results. Additional scans, across other diameters of
the detector, showed variations in the relative amounts of degradation
at different points around the periphery.

These observations can best be explained by the charge-loss mech-
anism illustrated in Fig. 6a. Here we have plotted the equipotential
lines for a top-hat detector under realistic assumptions for the sur-
face potential distribution. As indicated, there is a region at the
periphery of the detector where the internal field lines terminate on
the surface rather than the lithium n+ contact. Electrons produced
within the shaded area will be collected at the surface where they can
be trapped or recombined. Since the signal produced in the output
circuit by these electrons is related to the distance they travel, the
resulting signals are reduced in amplitude producing the observed low

energy background. It is apparent that the effect is more pronounced
for X rays which penetrate further into the crystal. The sensitivity
of the surface potential distribution to small changes is ambient con-
ditions explains the observed axial asymmetry in the background
degradation.

The imperfections described could be eliminated by collimation
of the incident radiation to avoid the peripheral region, but a far
more elegant solution is possible. Since the problem arises from a
distortion of the internal field lines near the surface of the sensi-
tive volume of the detector, we can define this boundary by using the
guard-ring detector structure shown in Fig. 6b. In this geometry,an
annular outer contact, or guard-ring, surrounds the active central
region. This guard-ring is biased at the same potential as the cen-
tral region resulting in the uniform potential distribution indicated
in the figure, thereby eliminating the surface problem. This can be
regarded as an electrostatic collimation technique, since the active
central region is defined by controlling the electric field profile
within the semiconductor crystal.

The background reduction realized by this method can be inferred
from the scanning data of Fig. 7. These are the results of scans per-
formed on a guard-ring detector--the data were obtained with the same
source-collimator, and are presented in the same format, as in Fig. 5;
the only difference is that the central region of the guard-ring detec-
tor is 6 mm in diameter. Although the peak/total behavior for ^{55}Fe
is not significantly changed, there is a large improvement in the ^{109}Cd
data near the edge of the sensitive region. The peak/total ratio for
^{109}Cd is now at its maximum value over nearly the full diameter of the
detector. The results of scans across other diameters of the detector
show identical behavior. When this peak/total is integrated over the
entire area of the detector, it represents approximately a factor of
10 reduction in the spectrum background.

Even this configuration suffers from partial charge losses at the edge of the central region. As shown in Fig. 8a, there is a small region at the boundary where the charge signal can be divided between the central region and the grounded guard-ring, resulting in a partial signal in the central region. This problem immediately suggests the solution in Fig. 8b where a signal is extracted both from the central region, and the surrounding guard ring. (A second outer guard ring is provided in order to reduce leakage currents in the inner guard-ring circuit.) When signals occur in both channels the output of the system is inhibited. The improved performance is illustrated in Fig. 9. Comparison of the ^{109}Cd data with that of Fig. 7 shows that the peak/total at the boundaries is improved with respect to the simple guard-ring system. Although the difference appears slight when presented in this format, a background reduction by a factor of four is realized when integrated over the entire detector area.

The importance of these background improvements in analytical applications is illustrated in Fig. 10, where we show a spectrum obtained under identical conditions to those of Fig. 4, but using the double guard-ring reject system. For comparison, the spectrum of Fig. 4 is also shown. The detection sensitivity is obviously improved with the double guard-ring system, particularly at the higher energies. This feature is important since the excitation efficiency with mono-energetic X rays is greatest for fluorescent X-ray energies just below the excitor energy.

The relative advantages of the double guard-ring detector system and a simple detector must be assessed in relation to the specific application considered. If only low-energy measurements (<5 keV) are to be performed, the scanning results quoted in this paper would indicate that the guard-ring detector has little to recommend it, as it requires more complex electronics than the standard detector. Similarly, in applications where there are sources of background with origins outside the detector, such as the Bremsstrahlung present in electron beam excitation, the reduction in detector background may not be important.

The misconception that the guard-ring detector inherently involves a sacrifice in energy resolution, is not correct, however, as shown in the ^{55}Fe spectrum shown in Fig. 11. The energy resolution (165 eV for Mn X rays and 99 eV pulser) is quite respectable for any system using a 6 mm diameter detector. The peripheral capacity of a guard-ring detector (less than 1 pF in this case), is apparently no larger than the excess capacitance introduced by surface states on the standard detector. This explains the comparable energy resolution obtained with the two detectors.

For higher-energy measurements, or where a broad energy range must be covered, the guard-ring system provides a <u>great</u> improvement as a realistic analytical tool to study trace elements, as compared with a system using any standard detector. The electronic collimation used in the guard-ring detector absolutely defines the sensitive volume without the use of external collimation. Therefore very efficient counting geometries can be used. Standard detectors, in order to achieve background levels approaching those of guard-ring detectors, must be of larger area (causing a penalty in resolution), and must use a high degree of collimation to limit the angular spread of incident X rays to within the central region. Neglecting for the moment the difficult problem of selecting a suitable material for a general purpose collimator, it is apparent that geometric restrictions on sample size and detector solid angle could lose as much as a factor of 100 in counting rate in realistic analytical problems. Compensating for this loss by using more intense excitation hardly seem a reasonable alternative to the electronic technique of the guard-ring system.

APPLICATIONS OF METHOD

To illustrate the applications of the X-ray fluorescence method, we have chosen three specific applications as examples of the types of biological and environmental problems that can be studied. Figure 12 is the fluorescence spectrum for a sample of freeze-dried whole blood obtained in a 10 min. count. The indicated concentrations refer to the original blood, and therefore represent concentrations in the freeze-dried sample approximately five times higher. The sample was prepared by compressing the freeze-dried powder into a thin wafer 1 inch in diameter, to ensure uniformity for calibration purposes. The measured lead concentration is several times the normal value, reflecting the fact that the sample was obtained from a child diagnosed as suffering from lead poisoning. The total volume of blood used is less than 2 ml--a sizeable reduction from the amounts required by current analysis methods. In addition to the lead determination, it is possible to obtain accurate measurement of the concentrations for other elements in the sample. Previous work on trace elements in blood has suggested correlations between these elemental concentrations and certain disease states.[5] The capabilities of modern X-ray fluorescence methods should permit more extensive studies of these and other correlations.

A second application of obvious environmental importance is the measurement of the elemental composition of particulate air pollutants. Figure 13 is a fluorescence X-ray spectrum obtained from an air filter which had been used to collect atmospheric particulates over a four hour period. The numbers on the spectrum refer to the concentrations of the elements on the filter in units of $\mu gm/cm^2$. The wide variety of elements observed demonstrates the advantage gained with the multielement detection capability. Correlation of elemental concentrations with natural, industrial and automotive sources could provide a useful

tool for environmental research and monitoring. An obvious example
is the determination of Pb and Br concentrations associated with atuo-
motive exhaust.

Figure 14 shows the results of a four-day study in which the Pb
and Fe concentrations in Berkeley were monitored in a series of air
samples taken over nominal two hour intervals. The exposed filters
were then analyzed for 10 min. in the X-ray fluorescence spectrometer.
Interesting correlations can be made between the lead and iron con-
centrations and qualitative weather observations. The first three
days (4/14 to 4/16) were weekdays, that could best be described as
relatively smoggy in terms of visibility and air movement. The week-
end of (4/17 and 4/18) was quite clear with moderate winds. The gen-
eral trends of both the lead and iron data correlate with these observa-
tions. The iron concentrations exhibit a regular diurnal cycle with a
maximum at midday, indicating predominance of industrial sources. The
lead concentrations also show a fine structure related to the weekday
rush hour traffic, and a peak late on Sunday evening due to returning
weekend travelers.

The final example concerns the application of the method to bio-
logical studies of trace-element effects in the marine ecology. Figure
15 is a fluorescence spectrum acquired in a 10 min. count of a mussel
sample. In this example the indicated concentrations refer to the
freeze dried sample, and are therefore five times greater than in the
original specimen. The abundance and variety of heavy elements in the
sample reflect the ability of certain species to concentrate environ-
mental pollutants. The presence of lead is especially important
because of its toxic effects. Figure 16 shows some preliminary results
of a survey of the mussel population in the San Francisco Bay Area.
The numbers on the map refer to the concentration of lead in samples
prepared from mussels collected at the indicated locations. The sam-
ples can be grouped into three categories on the basis of the measured
lead concentrations--the clean ocean environment with concentrations of

10 to 14 ppm, the Bay samples with concentrations of 20 to 40 ppm, and the one sample with 103 ppm, reflecting the proximity of this location to a lead smelter.

In each of the above examples, we have been able to demonstrate correlations between the measured trace-element concentrations, and certain biological or environmental factors. Considering the inherent accuracy and sensitivity of X-ray fluorescence spectrometers it is probable that more detailed studies of this type will result in increased understanding of the role of trace elements.

ACKNOWLEDGMENTS

REFERENCES

1. D. A. Landis, F. S. Goulding, R. H. Pehl and J. T. Walton, IEEE Trans. Nucl. Sci. Vol. SN-18 No. 1, 115 (1971).

2. J. M. Jaklevic, R. D. Giauque, D. F. Malone and W. L. Searles, "Small X-Ray Tubes for Energy Dispersive Analysis Using Semiconductor Spectrometers" presented at the 20th Annual Denver X-ray Conference, Aug. 11-13, 1971, Denver, Colorado. LBL-10 Lawrence Berkeley Laboratory report.

3. D. A. Gedcke, G. R. Dyer, and T. Harris, "Fluorescence Analysis Using a Si(Li) X-ray Energy Analysis System with Low-Power X-ray Tubes and Radioisotopes", presented at the 20th Annual Denver X-ray Conference, Denver, Colorado, Aug. 11-13, 1971.

4. F. S. Goulding, J. M. Jaklevic, B. V. Jarrett, and D. A. Landis, "Detector Background and Sensitivity of X-ray Fluorescence Spectrometers", presented at the 20th Annual Denver X-ray Conference, Denver, Colorado, Aug. 11-13, 1971. Lawrence Berkeley Laboratory report LBL-9.

5. J. W. Gofman, "Chemical Elements in the Blood in Health", in Advances in Biological and Medical Physics, Vol. 8 (1962) p 1 ed. C. A. Tobias, J. W. Lawrence (Academic) also UCRL-10211 p. 62; Semiannual Report, Biology and Medicine Donner Laboratory.

SAMPLE

EXCITATION

FLUORESCENT

X-RAYS

DETECTOR
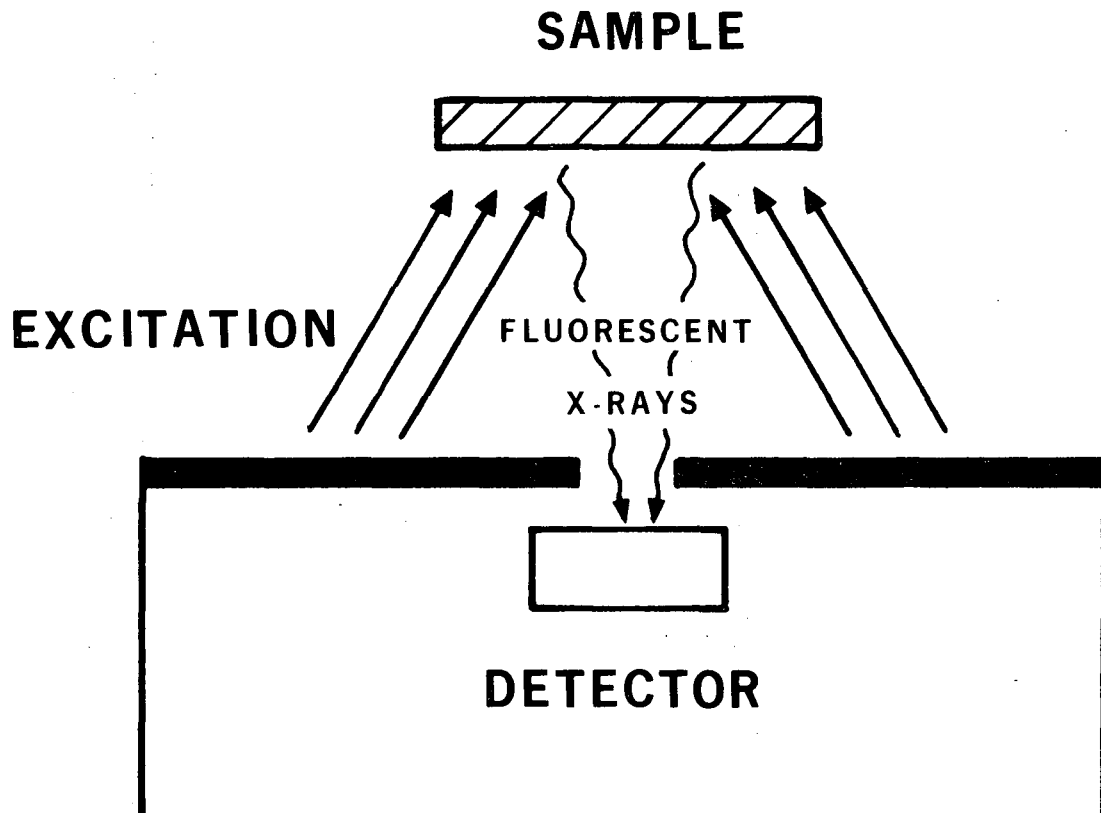
XBL 722-202

Fig. 1. Schematic of X-ray fluorescence
         method.
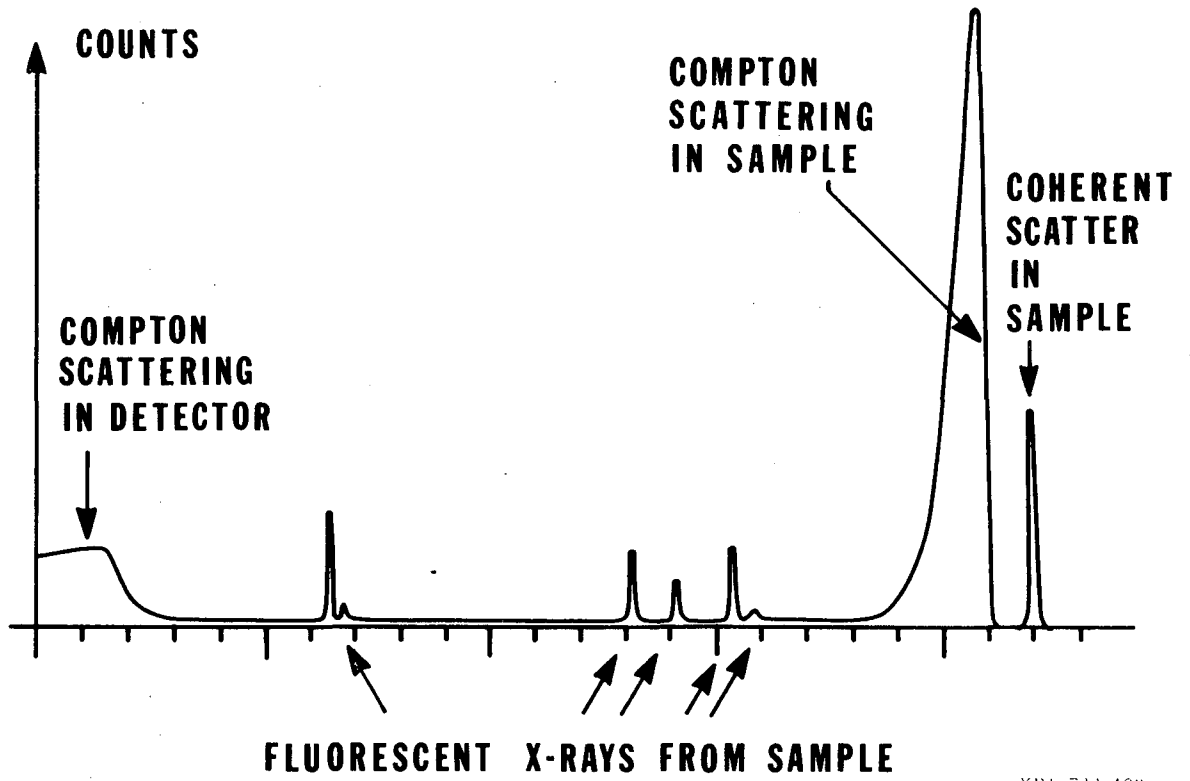
Fig. 2. Idealized spectrum observed by a
X-ray fluorescence spectrometer.
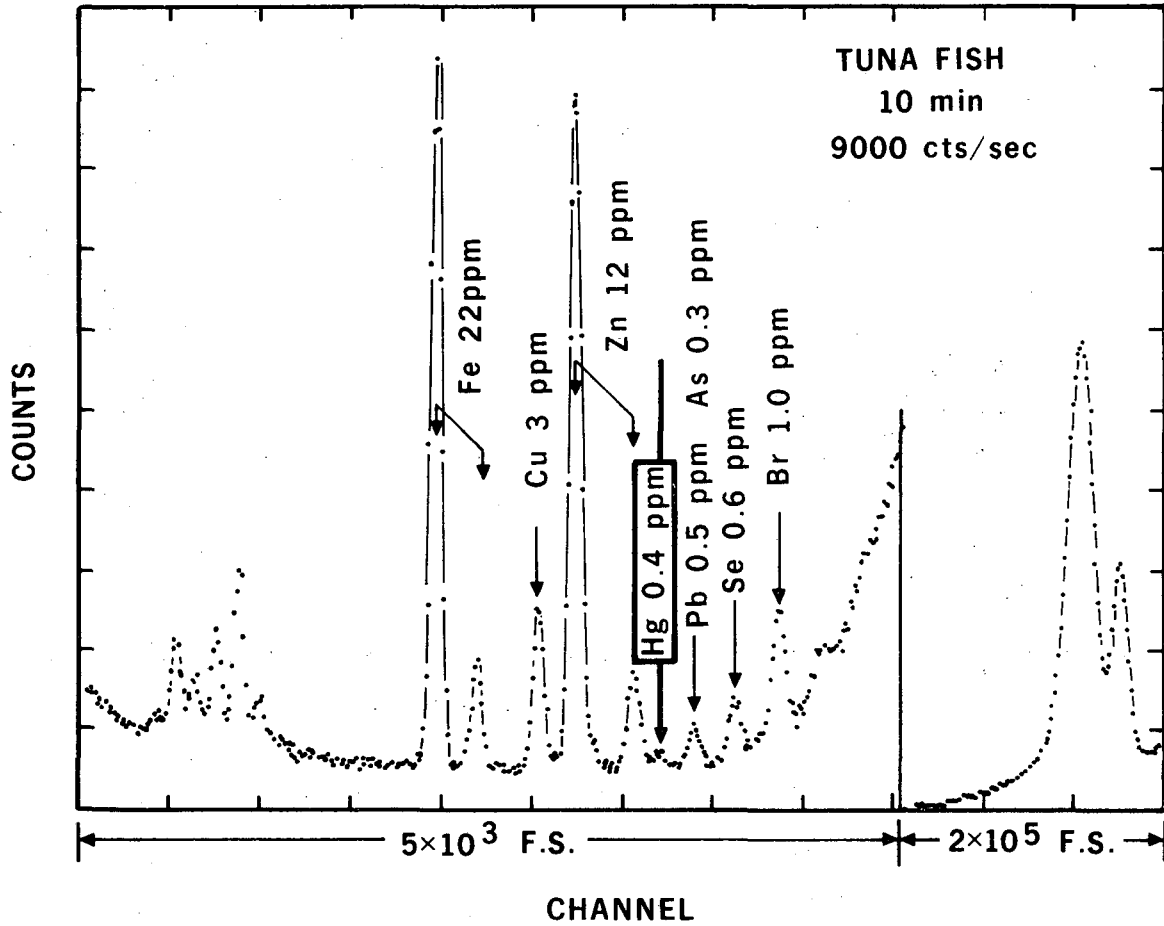
Fig. 3. X-ray fluorescence spectrum of tuna fish.
Concentrations in the dried sample are
five times higher than those indicated
on graph which refer to original fish.

BLOOD SERUM

TOP-HAT DETECTOR

COUNTS →

ENERGY keV → ← 5K FS | 500K FS →
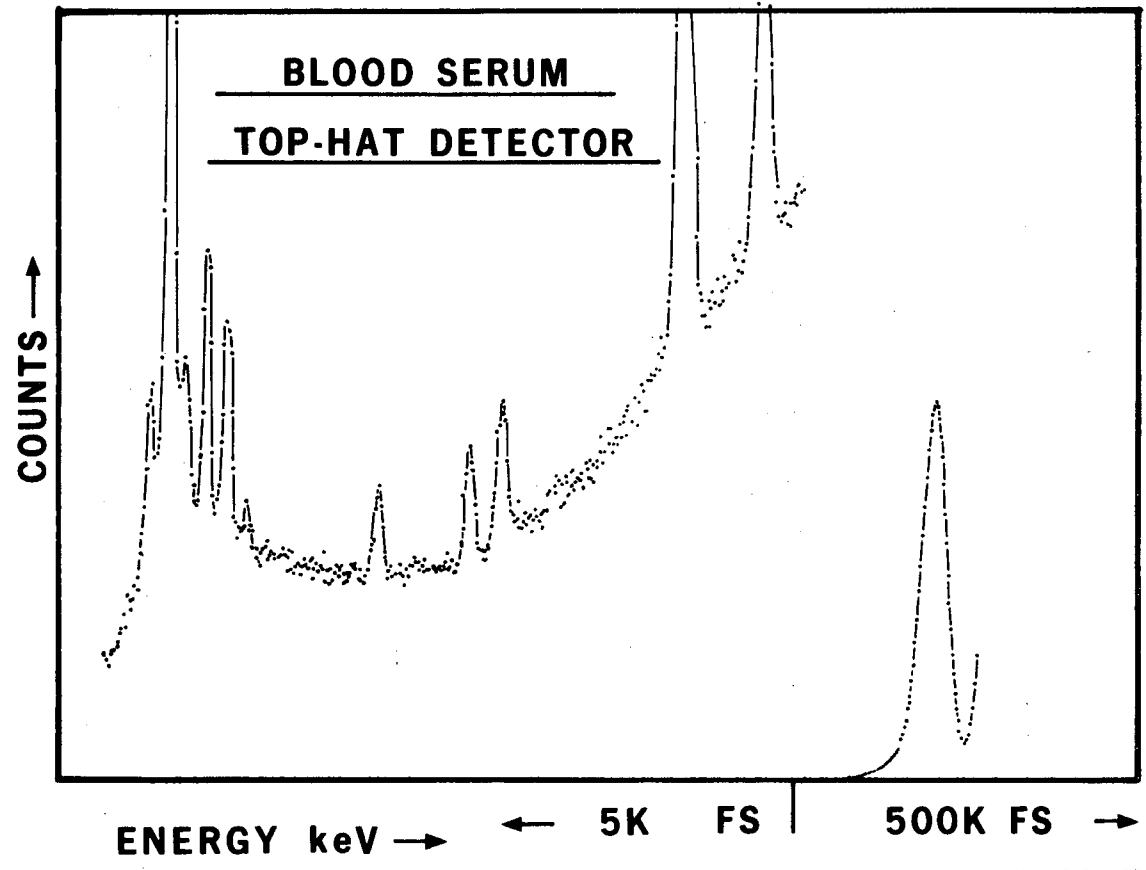
XBL 717-1177

Fig. 4. Fluorescence spectrum of a blood serum
sample obtained with a conventional
silicon detector spectrometer.

SCAN OF CONVENTIONAL DETECTOR
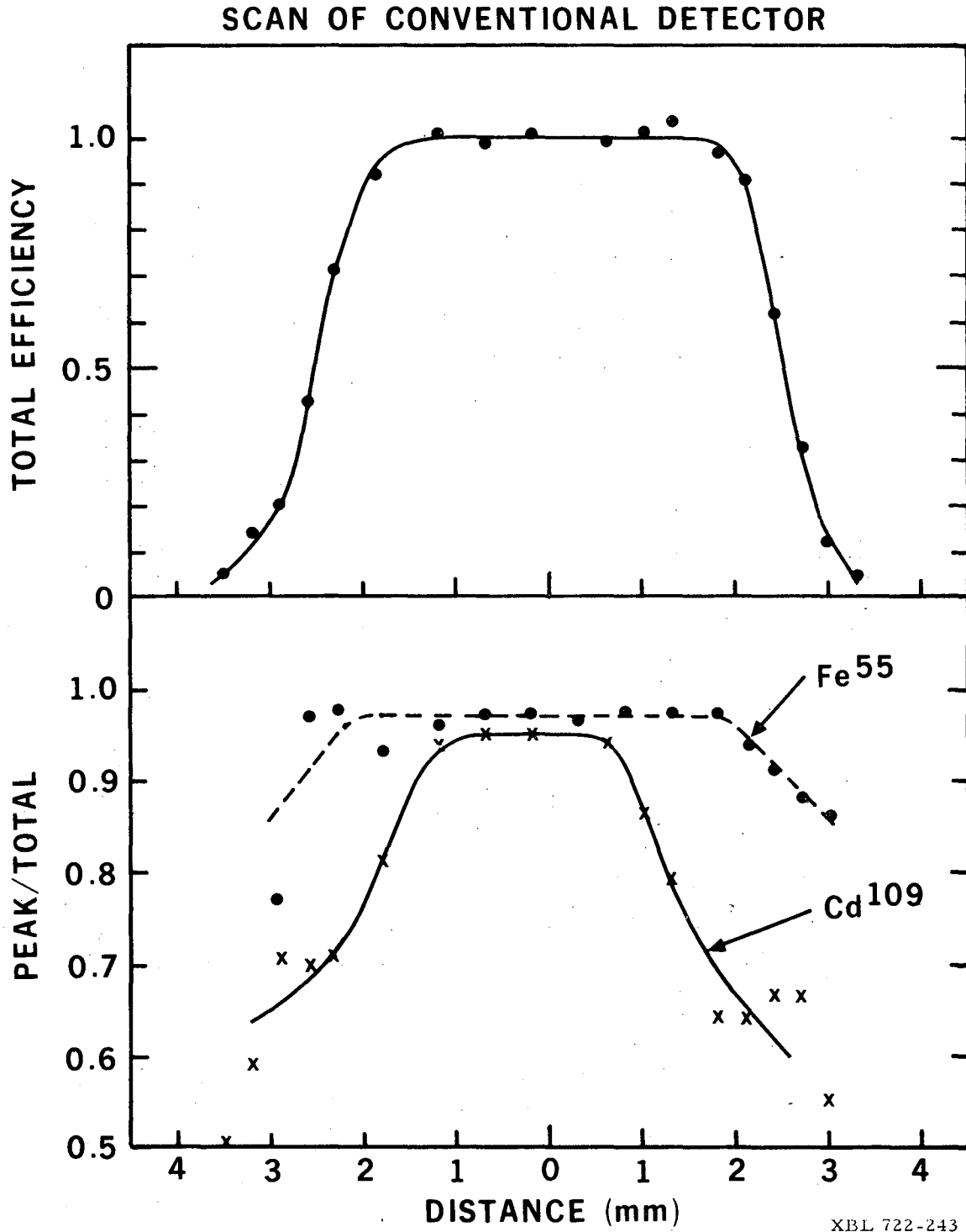
XBL 722-243

Fig. 5.   Results of detector scan. Collimator aperture
was 0.5 mm. Total efficiency refers to number
of counts in entire spectrum normalized to 1.0;
peak/total is ratio of K X-ray photopeak events
to the total.

Li-DIFFUSED LAYER (500V)

A.

CHARGE COLLECTED VIA SURFACE

HIGH-IMPEDANCE N-TYPE SURFACE CHANNEL

ORIGINAL P-TYPE MATERIAL

450
400
300
200
100
50

METAL SURFACE BARRIER

DRIFTED REGION

2mm

B.

500V   500V   500V

450
400
300
200
100
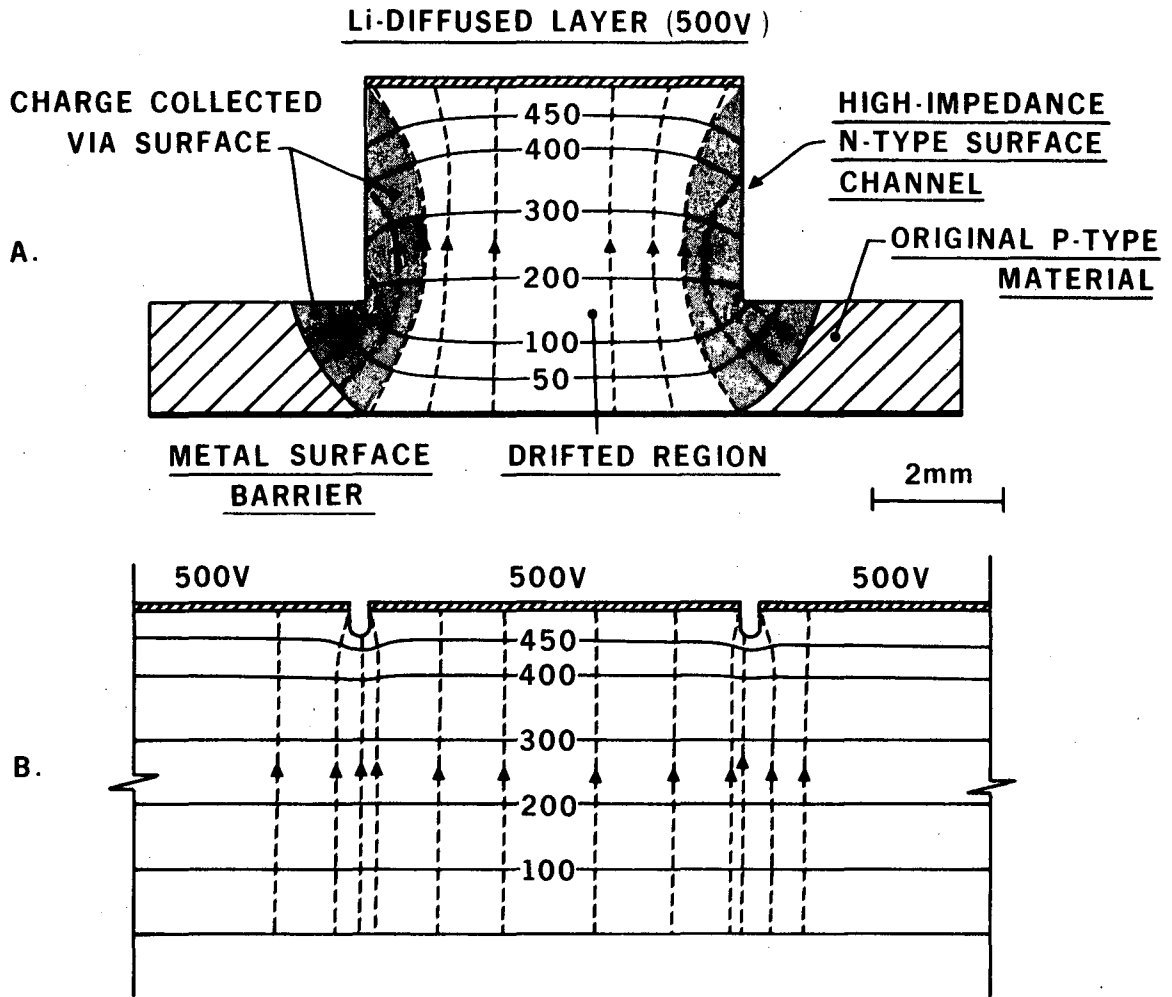
XBL 722-314

Fig. 6.   Internal electric field distributions of different detector geometries.

a)   Conventional top-hat detector. Shaded areas indicate region in which imperfect charge collection can occur.

b)   Guard-ring detector.

SCAN OF GROUNDED GUARD RING DETECTOR
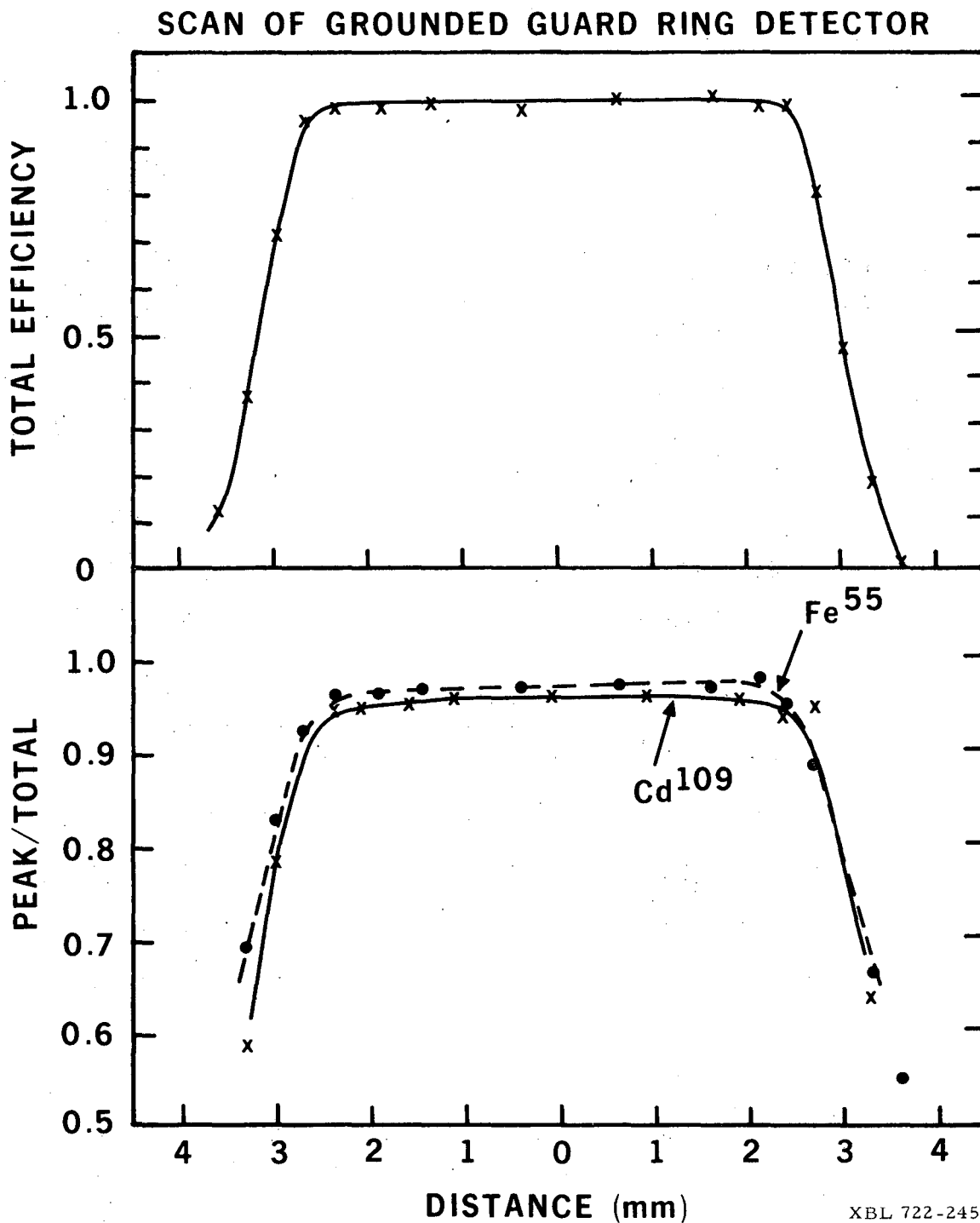
Fig. 7. Scan of guard-ring detector using same collimator as in Fig. 5.

FEEDBACK PREAMPLIFIER

a)

SIGNAL TO AMPLIFIER

C_F

DRIFTED REGION

GOLD SURFACE BARRIER

NEGATIVE DETECTOR BIAS

X-RAY

COINC. CCT.

b)

P.A.

FAST AMP. & DISC. 2

FAST AMP. & DISC. 1

ONE-SHOT

INHIBIT

P.A.

HIGH-RES. AMP.

LINEAR GATE

SIGNAL TO ANALYZER

NEGATIVE DETECTOR BIAS

XBL 717-1181
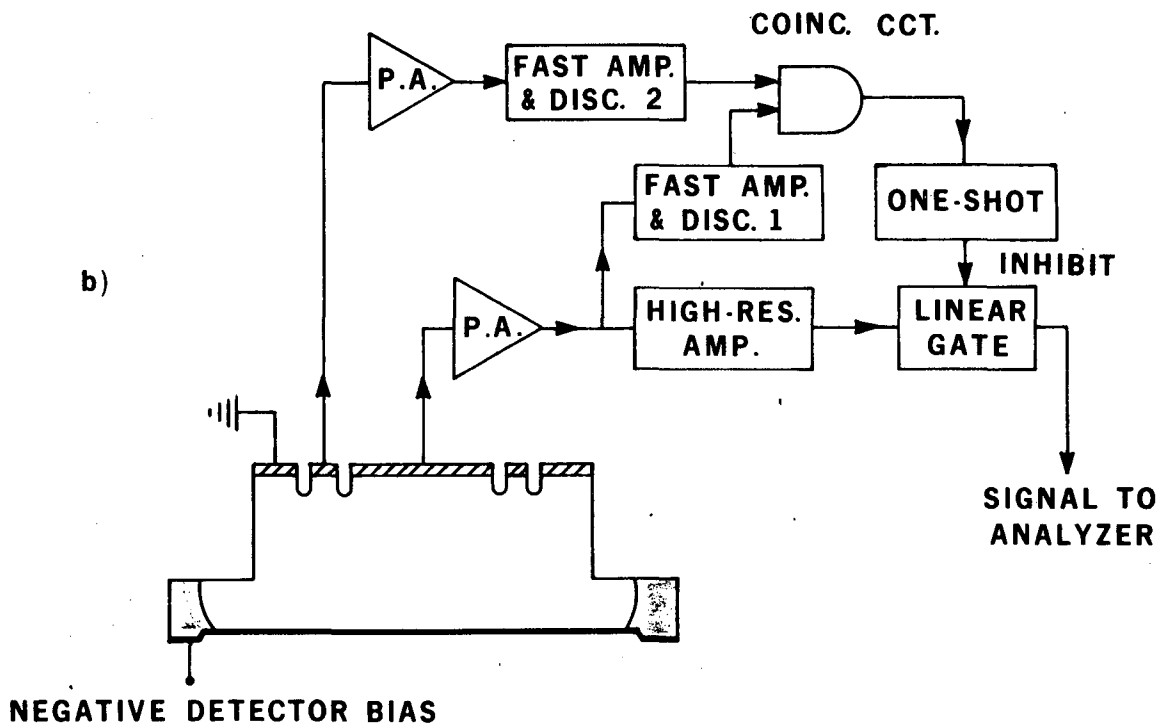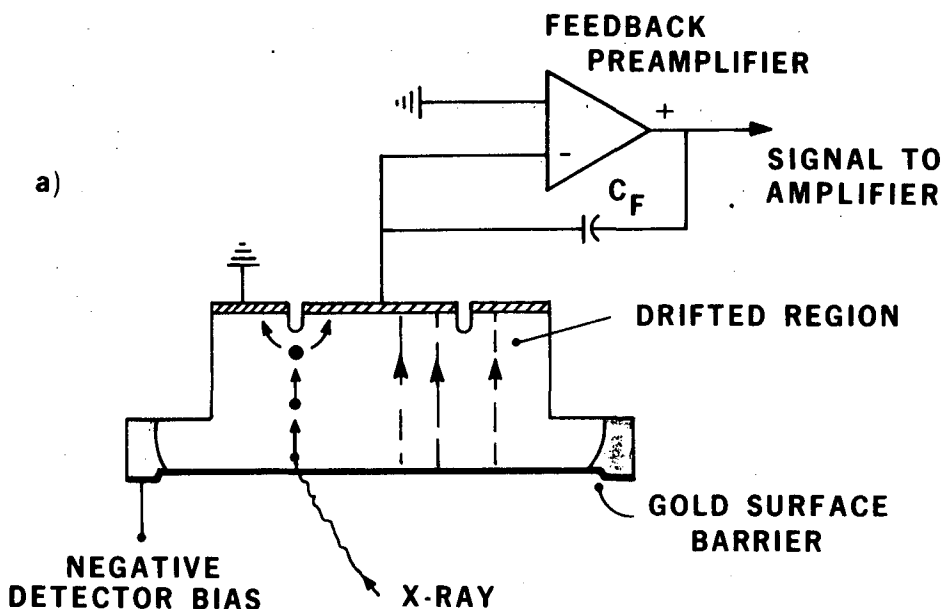
Fig. 8. Guard-ring detectors.

    a) Simple grounded guard ring approach showing the mechanism for degraded pulses.

    b) Double guard-ring detector with pulse-reject circuitry to remove degraded pulses.

SCAN OF DOUBLE GUARD RING REJECT SYSTEM
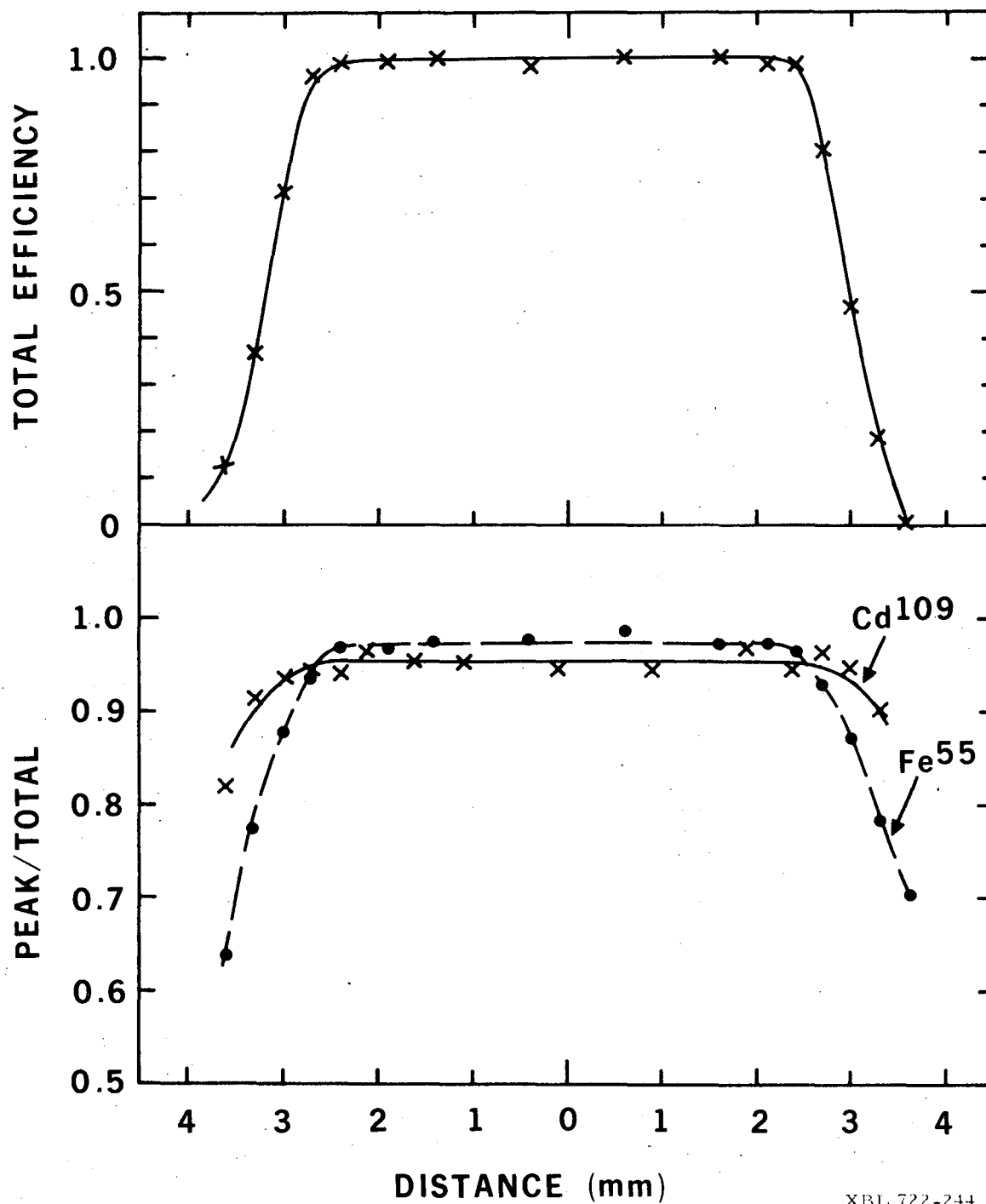
Fig. 9. Scan of double guard-ring detector.

XBL 722-244
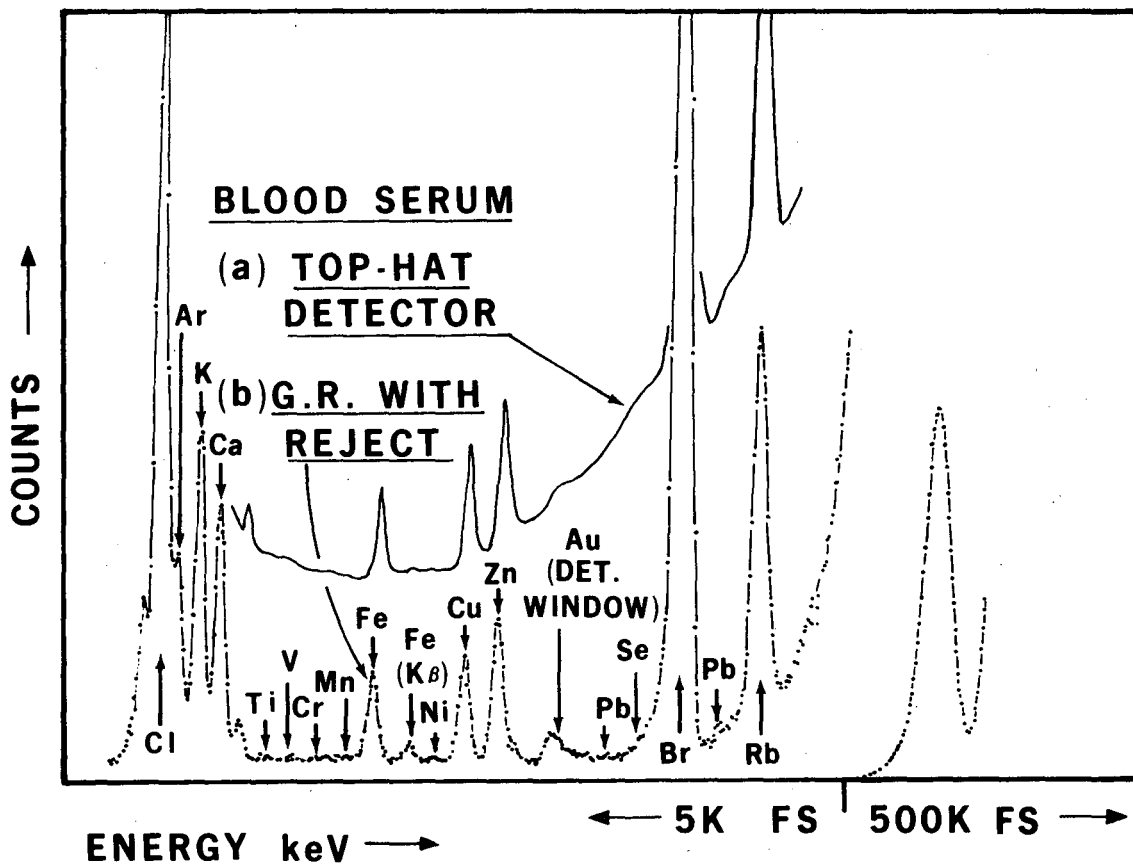
Fig. 10. Fluorescence X-ray spectrum obtained on a blood
serum specimen using a spectrometer equipped
with guard-ring detector and reject circuitry
(b). For comparison, the spectrum obtained on
the same sample with the same geometry, and the
same total counts in the scatter peak, but with a
conventional top-hat detector, is also shown (a).
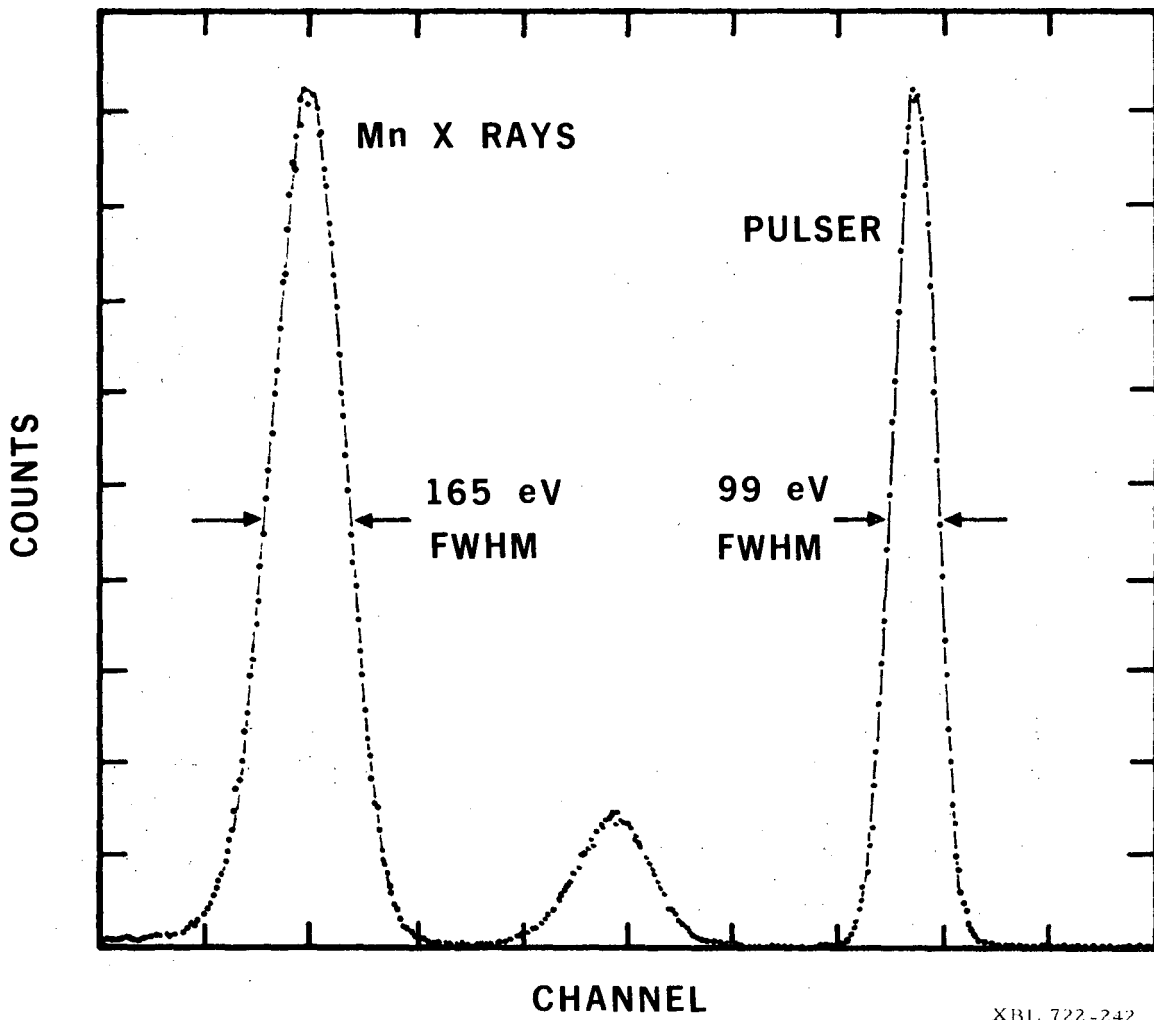
Fig. 11.   Mn X-ray spectrum obtained with
           double guard-ring detector.
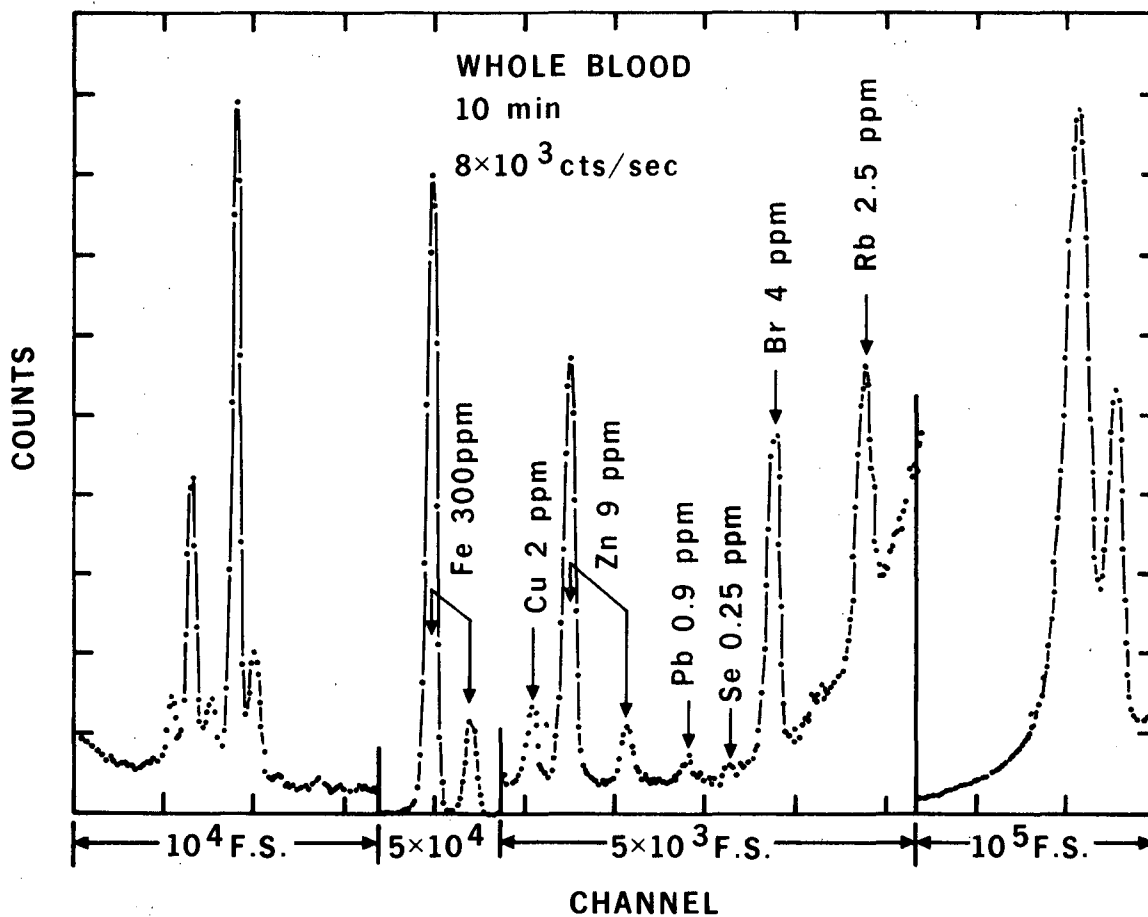
Fig. 12. X-ray fluorescence spectrum of whole blood.
The measured concentration of lead is
several times normal indicating lead poisoning.

XBL 722-345
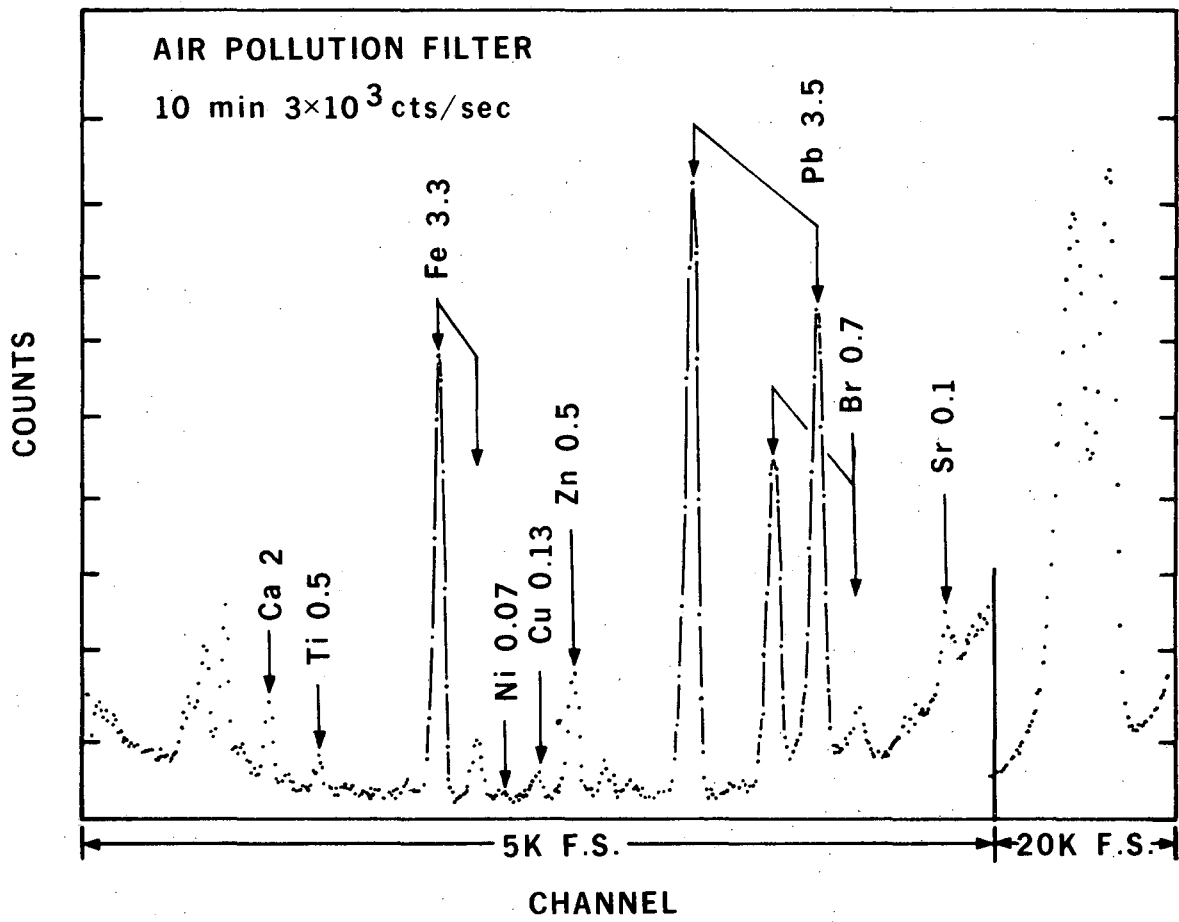
Fig. 13. Fluorescence spectrum of air pollution filter. Numbers are concentrations on the filter in μgm/cm².
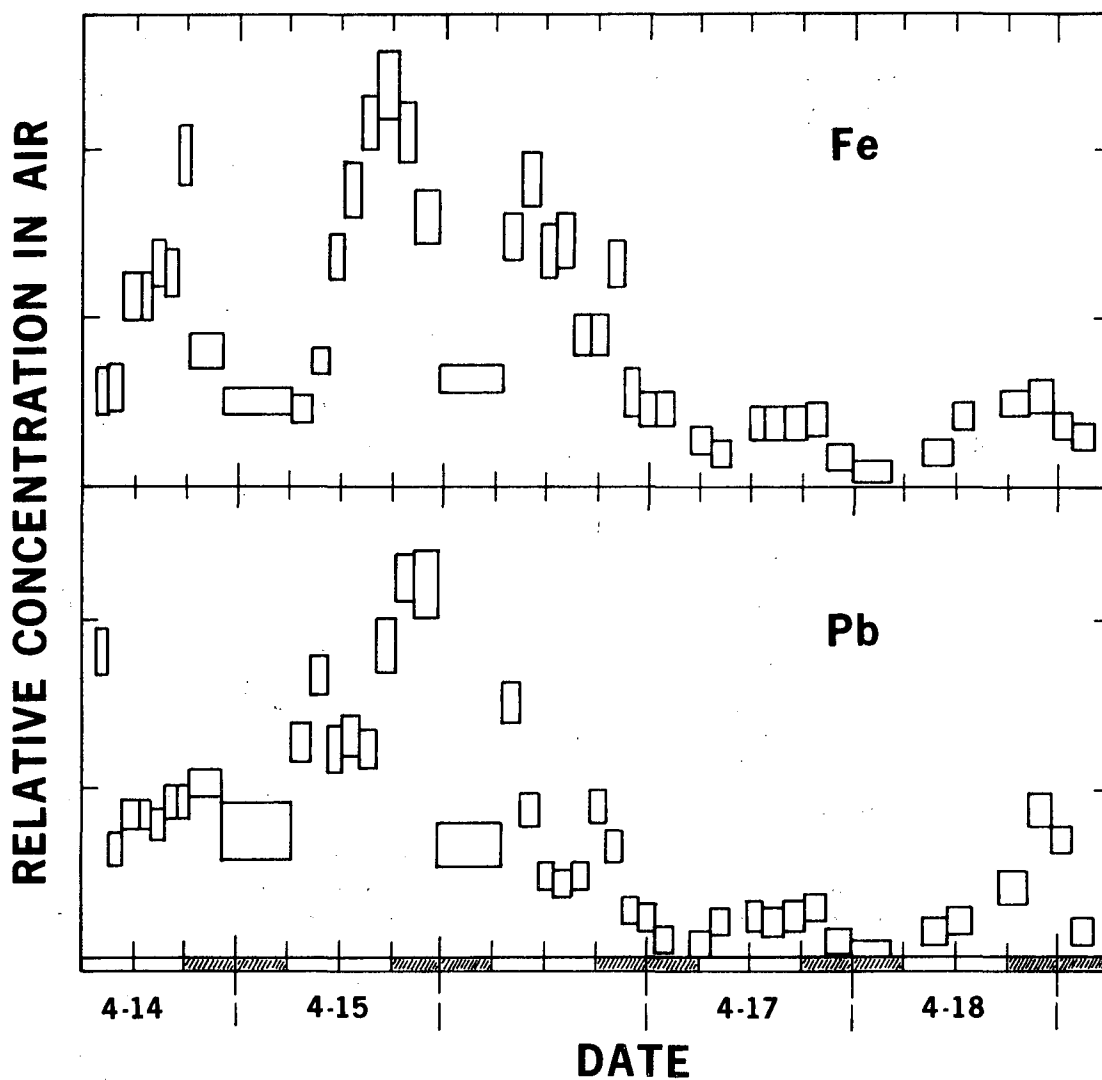
Fig. 14. Variation in atmospheric iron and
          lead concentrations in Berkeley as
          a function of time.
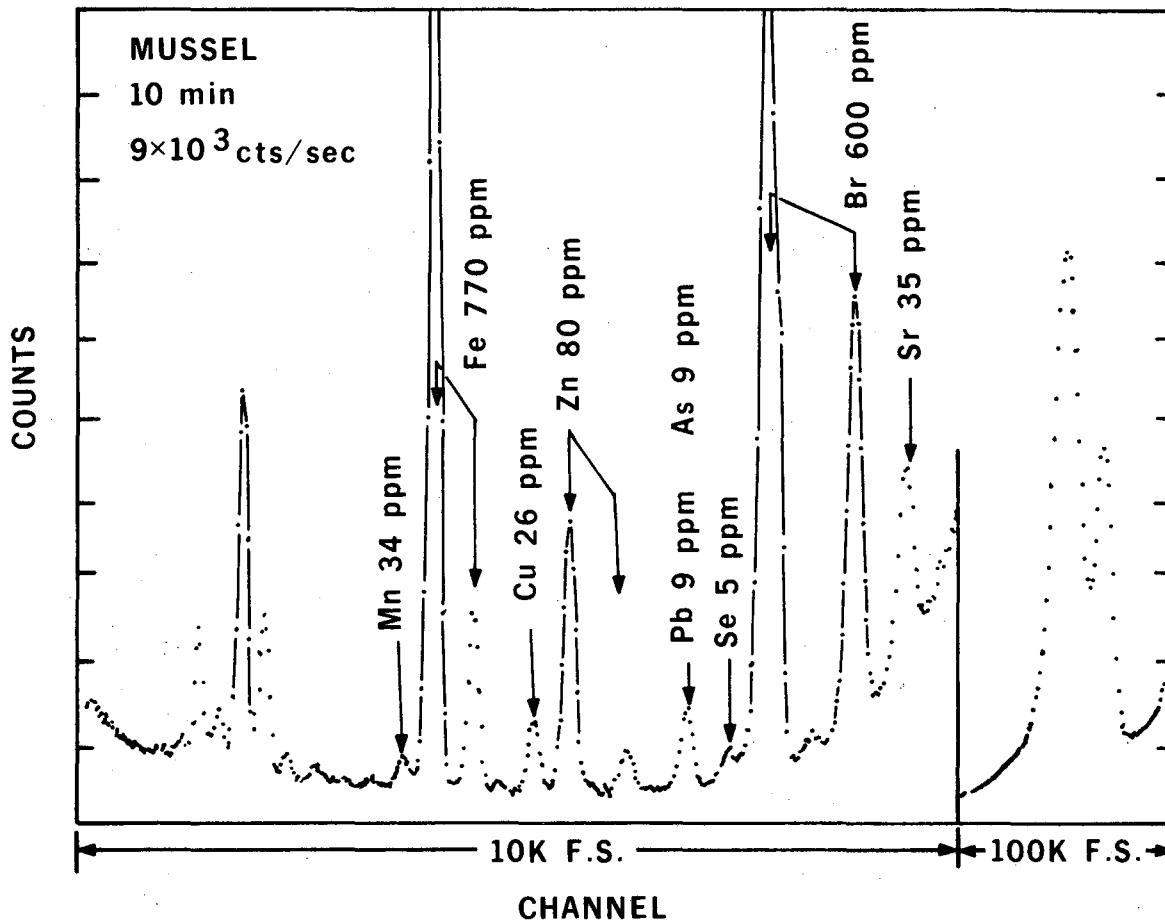
Fig. 15. Fluorescence spectrum of
          freeze-dried mussel.
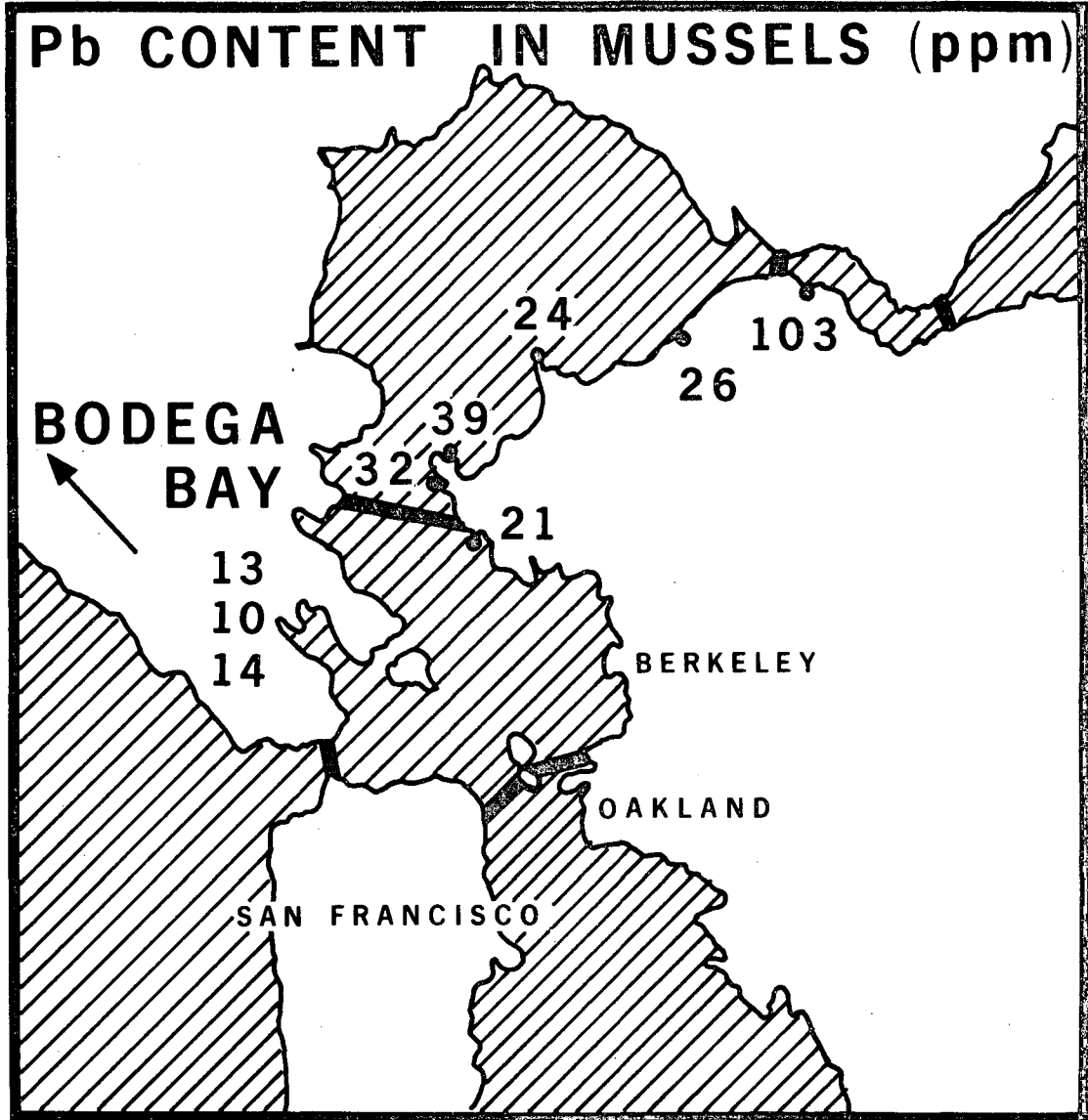
Fig. 16. Variation in Pb concentration in
mussels as a function of sampling
location.